Model, Analysis and Improvement of a Hydro Turbine Intake System

Liam Wood supervised by Dr Lian Gan

Abstract*—Hydropower has proven to be one of the most economically attractive forms of renewable energy. The Archimedes Screw Turbine (AST), has played a considerable role within hydropower technology over the last decade, and research into this area is plentiful. However, studies investigating the intake system are scarce, with little research into how the intake system can be improved. This project aims to look at the existing intake system of an AST based in Ruswarp, Whitby. The project will model the intake system and modify the design using ANSYS Fluent 15.0. Results show that the current intake system is developing a substantial amount of turbulent kinetic energy from the corners, which is resulting in a pressure head loss. The design changes were shown to increase the total pressure and the maximum velocity magnitude which should lead to an increase in energy production. However, results showed that the design changes did not reduce the maximum turbulent kinetic energy compared to the current intake design. Nevertheless, positive results have been seen using an area – weighted average for the total pressure loss and turbulent kinetic energy from the inlet and outlet. This project therefore, has shown that minor design changes can make a significant difference to the fluid flow throughout the inlet system.

***Index Terms*—ANSYS Fluent 15.0, Hydro-Turbine, Intake System, K-[epsilon] Model**

I. INTRODUCTION

Hydropower has been shown to be a more economically attractive from of renewable energy than other available options [1]. For this reason, it has played, an indispensable role within the advancement of humanity [1], [2]. Hydropower is a very simple concept which takes free-falling water and converts it into electricity by using the available "free" kinetic energy [3]. The water that passes through the turbine, causes the rotation of a generator, producing electricity to be then transferred to the grid.

There are three main types of hydropower: impoundment, diversion and run-of-river (RoR). This project focuses solely on RoR which utilises the natural water flow of a low-head river [4]. This method produces a continuous power outflow as it is relative to the steady inflow velocity of the stream [5]. This simplistic process can enable electricity to be generated at efficiencies of up to 85-95% [5]. The turbines used in the RoR classification are known as micro-hydropower, because of the smaller size of the turbine which range between 50-100kW [6]. This method has less environmental impact compared to large-scale-hydropower, known as impoundment, which includes structures such as dams [7]. The Archimedes Screw Turbine (AST), is becoming increasingly common, due to its high efficiency and low environmental impact [8]. Radlik conducted experiments which showed AST turbines could perform at efficiencies of up to 84.5% [9]. Since then, this method for generating electricity has been widely used for rivers with a depth between 1-6m. It has been shown that at the lower depths the energy generation works at a higher efficiency due to the faster flow of water [9].

The intake system to these types of turbines work as a guide for the water as it is diverted from the main course of the river. The aim of these intake systems is to minimise the total head loss [m], ensuring that the water level is kept constant. As a result, this causes the turbine to run at a higher efficiency as the water entering is at a higher total pressure [Pa]. Therefore, it is essential that the inlet system is contributing to as little head loss as possible. Extensive amounts of research have been conducted on the design of the AST, which has ensured the power output is maximised fully. This research has been conducted either by use of computational fluid dynamics (CFD), or by using scaled down models of existing turbines [10], [11], [12]. However, currently there has been very little research regarding the intake system, and how this can be maximised to ensure higher efficiency leading to increased electrical generation.

The aim of this project, in collaboration with Whitby Esk Energy, is to investigate the intake system of an AST located on the River Esk. This turbine is located on a tidal river, which flows into Whitby harbour. The turbine is placed to the side of the river and water flows from the main body of water into the inlet system. At the point in which the turbine is located, the river is around 20 [m] wide and 3 [m] in depth. The flow rate of the river varies seasonally, with the maximum flow rate in Spring recorded as 75.2 [m^3/s]. Often during the summer periods the volumetric flow rate of the river is too low and therefore the turbine is not operational. Attached to the turbine is a fish pass, which allows for safe passage of any fish down the weir. Images of the turbine can be found in Figure 1.

The inlet system is manufactured out of six solid concrete blocks, with a concrete base. This material prevents plant life from growing within the inlet

system. The inlet screens which prevent debris entering the inlet system are manufactured from steel and the angle of the screens can be individually adjusted manually. There are in total forty (five groups of eight) guide vanes which span across the entire mouth of the inlet system, indicated by Figure 1b.

Figure 1- Images provided by Whitby Esk Energy. The Intake System with a View of the Fish Pass (a). The Inlet Screens at the Mouth of the Intake System (b).

This thesis aims to model the current intake system design using SolidWorks 2016/17, and simulate the flow using ANSYS Fluent 15.0.

Once modelled the total pressure loss [Pa] and turbulent kinetic energy (K) [m^2/s^2] of the inlet system can be observed. Following this, the existing design will be modified with the aim of reducing these parameters across the intake system. The experimental hypothesis for this project is that the modified intake system design will significantly decrease the turbulent kinetic energy, increase the total pressure and velocity magnitude, compared to the original inlet system design. Increasing the total pressure will lead to a decrease in total pressure loss across the intake system.

II. THEORY

There are many different formulae used to support the theory behind how a turbine produces electricity. One formula is a general equation that allows the power (electricity) available from the turbine to be calculated. This is relative to the efficiency, volumetric flow rate and the pressure head [6].

$$P = \eta.\rho.g.Q.H \quad (1)$$

Where P is the mechanical power output [W], η is the efficiency of the turbine [%], ρ is the standard density of water [kg/m^3], g is the gravitational constant 9.81 [m/s], Q is the volumetric flowrate of the river [m^3/s] and H is the pressure head [m] [6].

Fluid dynamics is a practical way of understanding how a liquid or gas reacts within different environments. Computational Fluid Dynamics (CFD) takes a complex fluid flow scenario and enables the user to identify and understand how a flow reacts under certain conditions, using aid from numerical based software's [13]. Two main equations used, acquired from the Navier Stokes equations utilised within CFD, are the Conservation of Mass (Equation 2) and Momentum (Equation 3).

$$\frac{d}{dt}\int_{V(t)} \rho(x,t)\,dV = \int_{V(t)} \sigma(x,t)dV \quad (2)$$

$$\int_{V(t)} \rho\frac{Du_i}{Dt} = \int_{V(t)} \rho F_i dV + \int_{S(t)} R_i dS \quad (3)$$

Laminar and turbulent flow are two very important concepts to consider within CFD. Figure 2 gives a visual representation of a simple simulation of laminar and turbulent flow within ANSYS Fluent 15.0. Figure 2a is known as laminar flow. This occurs when there are no disturbances to the flow within a pipe or vessel. Figure 2b however, gives a visual representation of turbulent flow. By adding a small disturbance to the pipe or vessel centre, the flow is disturbed causing vortices behind the design alteration. Figure 2b also shows that the flow is recirculating after the alteration. This can be seen by the red patch on the image. This implies that there is a large amount of turbulent kinetic energy within the flow, having an impact on varying outputs. This will occur until the flow returns to a laminar state.

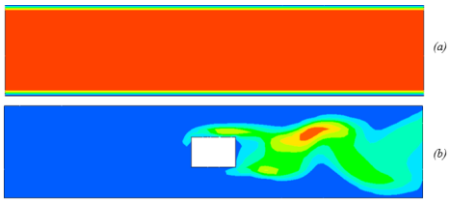

Figure 2 - A Depiction of Laminar Flow at 1m/s (a) and a Depiction of Turbulent Flow at 1m/s (b)

Turbulent flow creates vortices in the water flow, especially around sharp corners [14]. The research into this has been considerable, particularly over the last two decades. This research has allowed for an understanding of how designs can be modified to reduce turbulent flow across different models [14]. The foundation of turbulent modelling on a two-parameter basis uses the Reynold's averaged Navier-Stokes equations, (RANS) [15]. To obtain the RANS equation, the solution variables within the Mass and Momentum Conservation Navier-Stokes equations are separated into two distinct mean and fluctuating components for velocity and pressure respectively

[16]. Where $\bar{u}_i$ and u'_i are mean and fluctuating velocity components, and $\emptyset$ represents a scalar model (i.e. pressure) [16].

$$u_i = \bar{u}_i + u'_i \quad (4)$$

$$\emptyset = \bar{\emptyset} + \emptyset' \quad (5)$$

The steady state Reynolds's averaged Navier-Stokes (RANS) equations, can be then written in Cartesian tenser form [16].

$$\frac{\partial \rho}{\partial t} + \frac{\partial}{\partial x_i}(\rho u_i) = 0 \quad (6)$$

$$\frac{\partial}{\partial t}(\rho u_i) + \frac{\partial}{\partial x_j}(\rho u_i u_j) = -\frac{\partial P}{\partial x_i} + \frac{\partial}{\partial x_j}\left[\left(\mu \frac{\partial u_i}{\partial x_j} + \frac{\partial u_j}{\partial x_i} - \frac{2}{3}\delta_{ij}\frac{\partial u_l}{\partial x_l}\right)\right] + \frac{\partial}{\partial x_j} - \overline{\rho u'_i u'_j} \quad (7)$$

The parameters within the equations are set so ρ is the density of a fluid, t is the time taken, U_i and U_j are classed as the mean velocity components in the direction coordinates of x_i and x_j respectfully, P is the pressure, μ is the dynamic viscosity and u' is a fluctuation of the velocity [17].

Within Equation 7, the terms $-\overline{\rho u'_i u'_j}$ are known as the Reynold's stresses [18]. When implementing the Reynold's stresses, the most widely used concept is to introduce an eddy viscosity utilising the Boussinesq Hypothesis [18].

$$-\overline{\rho u'_i u'_j} = \mu \frac{\partial u_i}{\partial x_j} + \frac{\partial u_j}{\partial x_i} - \frac{2}{3}\delta_{ij}\left(\rho k + \mu_t \frac{\partial u_k}{\partial x_k}\right) \quad (8)$$

When implementing CFD, there are several different turbulent models that can be used. These are either classified as one or two-equation models, where the two-equation model is the most common regarding its capability to achieve high quality numerical results [13], [16]. Within the different methods of modelling turbulent flow, two models have been considered. These are, K-[epsilon] model and the K-[omega] model. Where K is the kinetic energy, epsilon is the turbulent dissipation rate and omega is the specific dissipation rate [15].

K-[epsilon] Model (Launder-Sharma)

The K-[epsilon] model is a commonly used two-equation model when working on different CFD simulations, and has played a large role within fluid flow research [19], [13]. Within this model, there are two transport variables, K, and, ε, which are solved. These respectfully are known as the turbulent kinetic energy and the turbulent dissipation rate.

The K-[epsilon] model, in the range of free-shear-layer flows within the incidence of small pressure gradients, has produced respectable results within the past [20]. The model has been outlined as a strong contender within CFD as it is able to solve an extensive range of turbulent flows [19].

This model proposes that the turbulent viscosity is related to the turbulent kinetic energy and turbulent dissipation rate by the following equation, where C_μ =0.09. [13].

$$\mu_t = C_\mu \rho \frac{k^2}{\varepsilon} \quad (9)$$

There are, following this, two transport equations used to solve the turbulent kinetic energy and turbulent dissipation rate respectively [19].

$$\frac{\partial(\rho k)}{\partial t} + \frac{\partial}{\partial x_i}(\rho U_i k) = \frac{\partial}{\partial x_i}\left(\mu + \frac{\mu_t}{\sigma_k}\right)\frac{\partial k}{\partial x_i} + G_k - \rho\varepsilon \quad (10)$$

$$\frac{\partial(\rho\varepsilon)}{\partial t} + \frac{\partial}{\partial x_i}(\rho U_i \varepsilon) = \frac{\partial}{\partial x_i}\left(\mu + \frac{\mu_t}{\sigma_\varepsilon}\right)\frac{\partial \varepsilon}{\partial x_i} + C_1 \frac{\varepsilon}{k} G_k + C_2 \rho \frac{\varepsilon^2}{k} \quad (11)$$

Within the equations, there are empirical constants throughout the models which can be defined as: C_μ = 0.09, C_1 = 1.44, C_2 = 1.92, σ_k = 1.0 and σ_ε = 1.3 [20]. The value G_k can be characterised within both equations as a value for turbulence [19]. From Equation 12, the value for turbulence influences products of velocity gradients and is determined by the turbulent viscosity within the model [19].

$$G_k = \mu_t \left(\frac{\partial U_i}{\partial x_j} + \frac{\partial U_j}{\partial x_i}\right)\frac{\partial U_j}{\partial x_i} \quad (12)$$

Once the empirical values for turbulent kinetic energy and the turbulent dissipation rate have been computed using Equations 10 and 11, the turbulent viscosity can then be utilised, and the Reynold's stresses can be found through the Boussinesq Hypothesis [19].

K-[omega] Model (Wilcox)

The K-[omega] model was developed independently by Kolmogorov, with the research being continued by Wilcox, improving the model over the past three decades [21]. During this time, the model has demonstrated an improvement in accuracy within a wide range of turbulent flows [21].

Like the K-[epsilon] model, the K-[omega] model is defined by a relationship between turbulent viscosity, associated to the turbulent kinetic energy and the specific dissipation rate [13].

$$\mu_t = \rho \frac{k}{\omega} \quad (13)$$

The transport equations are then as follows for the turbulent kinetic energy and specific dissipation rate respectfully [13].

$$\frac{\partial(\rho k)}{\partial t} + \frac{\partial}{\partial x_j}(\rho U_j k) = \frac{\partial}{\partial x_j}\left[\left(\mu + \frac{\mu_t}{\sigma_k}\right)\frac{\partial k}{\partial x_j}\right] + P - \beta' \rho k \omega \quad (14)$$

$$\frac{\partial(\rho\omega)}{\partial t} + \frac{\partial}{\partial x_j}(\rho U_j \omega) = \frac{\partial}{\partial x_j}\left[\left(\mu + \frac{\mu_t}{\sigma_\omega}\right)\frac{\partial \omega}{\partial x_j}\right] + \alpha \frac{\omega}{k} P - \beta \rho \omega^2 \quad (15)$$

Referring to Wilcox, the constraints of the model are defined as: α = 5/9, β = 0.075, β' = 0.09, σ_k = 0.5 and σ_ω = 0.5 [20].

Chosen Turbulent Model (K-[epsilon] Model)

Due to the nature of this project, the type of turbulent model that will be applied to the simulation of the intake system to the AST will be the K-[epsilon] model. Using however, the Boussinesq Hypothesis to calculate the turbulence within a model, does have a

small effect on the accuracy of the simulation [18]. Other forms of turbulent simulation such as Direct Numerical Simulation (DNS) and Large Eddy Simulation (LES) are more accurate when conducting a turbulent calculation, the computational cost is too high [18]. Therefore, the Reynold's Averaging Navier-Stokes (RANS) turbulent models will be used within this project as they have been used within many different engineering turbulent models. This is due to the nature of the simulation and low computational cost providing a representation of the nature of a flow [18].

Within the K-[epsilon] model, there are different variants concerning the type of turbulent calculation. The first is the Standard K-[epsilon] model which has been demonstrated above by Equations (10), (11). However, throughout its time, the model has been referred to as "inaccurate" by many researchers when calculating turbulent flows [22]. The second is the Re-normalisation Group (RNG) K-[epsilon] model [15]. It has been recorded that at high Reynold's values for turbulence, the RNG K-[epsilon] model works in a similar manor as the Standard K-[epsilon] model, with slight variations to the turbulent kinetic energy and turbulent dissipation rate equations [23]. The final model is the realizable K-[epsilon] model. Within CFD, realizable implies that the simulation fulfils numerous mathematical parameters [15]. This turbulent model, along with the RNG model have, in the past, shown greater improvements than the standard K-[epsilon] model [16]. It has also been demonstrated that the realizable K-[epsilon] model provides the best turbulent results against all the previous K-[epsilon] models [16]. From a comparison of the different model variants, the simulation will be based off the realizable K-[epsilon] model.

III. METHODOLOGY

Firstly, the existing design of the intake system was modelled within SolidWorks 2016/17. This was to ensure the accuracy of the geometry, compared with the drawings provided. In the model, the total number of inlet screens will be reduced to eight. This is because modelling and simulating forty inlet screens would increase computational time and cost. Even with the reduced number of guide vanes, the overall results will not be dis-similar. This affect has been noted and any conclusions drawn from the models will consider this with future studies.

The drawings will then be transferred into ANSYS Fluent 15.0, which will be used as the basis for the flow simulations. The existing engineering drawings for both the intake system and the inlet screens can be found in Appendix A and B respectively.

When using ANSYS Fluent 15.0 a mesh must be generated for the model, to ensure accuracy in the simulation. The creation of the mesh is characterised as one of the most time consuming and important processes within CFD [24]. The mesh will be refined with a greater number of nodes and elements to ensure a higher accuracy [24]. Therefore, where higher turbulent energy and total pressure is likely to be seen, more accurate results can be produced. In the centre of the inlet system there is less need for high levels of refinement, as the flow in the centre of the inlet system is less turbulent. This subsequently, reduces the computational cost, as the simulation converges within a reasonable time scale.

Before starting the initial simulation setup, a quality report for the mesh will be calculated. This will ensure that the mesh generated is appropriate for the simulation by producing an orthogonal quality value. The orthogonal quality value is a number ranging from 0 to 1 [24]. It states that if the value is low, then the mesh is of lower quality [24].

When initiating the simulation, boundary conditions must be set for the model. The first boundary condition is the velocity inlet. The velocity has been calculated using the maximum value for the volumetric flow rate of the River Esk at the site of the turbine. This information is readily available and updated daily on Whitby Esk Energy's website. The volumetric flow rate was recorded over April 2018, and the highest value taken was 75.2 [m^3 /s]. The lowest volumetric flow rate recorded in June 2018, was taken as 0.09 [m^3 /s]. From these two values, and knowing the frontal area of the inlet system, the maximum and minimum velocities have been calculated as 6.776 [m/s] and 0.08 [m/s] respectively. The second parameter variant regarding the inflow velocity is the turbulent intensity which is characterised as a percentage of turbulence. To optimise the simulations, the turbulent intensity will be altered between 10 [%] and 20 [%] for both the high and lower velocities respectfully. The final boundary condition is the outlet, which will be analysed as a pressure outlet where the only parameter effected is the turbulent intensity (this is to match the turbulent intensity at the inlet). Gauge pressure is not altered within the setup as the intake system is an "open tank vessel". This implies that the gauge pressure is zero-referenced against ambient air pressure. The solution method will also be modified where appropriate for the basis of the simulation. The spatial discretization will be set to the following settings: gradient – Least Squares Cell Based, pressure – Second Order. Following this, the momentum, turbulent kinetic energy and turbulent dissipation rate will all be set to Second Order Upwind. This is a more accurate representation for the parameters [24].

Once the inlet system is fully initialised, the following parameters will be calculated at both the high and low velocity flows: total pressure [Pa], velocity magnitude [m/s], turbulent kinetic energy [m^2/s^2], turbulent dissipation rate [m^2/s^3], turbulent intensity [%] and turbulent viscosity [kg/m-s]. Using these results, several design changes will be produced, which aim to improve the flow of water through the inlet system. Results for the stated parameters will then be calculated for each design change and the area – weighted average will also be determined. The area – weighted average is calculated by dividing the total sum of the inlet and outlet variables and their

corresponding areas by the total area of the design [16]. This provides a representation of the total pressure loss and the total kinetic energy, by taking integrated values from the inlet and outlet. Finally, an average figure of the two is calculated and shown as the total face value. This will be calculated for total pressure loss and turbulent kinetic energy.

These design changes will be analysed using statistical analysis to determine which design leads to the greater increment in fluid flow.

IV. RESULTS

The mesh was generated for both the existing design with and without the inlet screens, and each design modification.

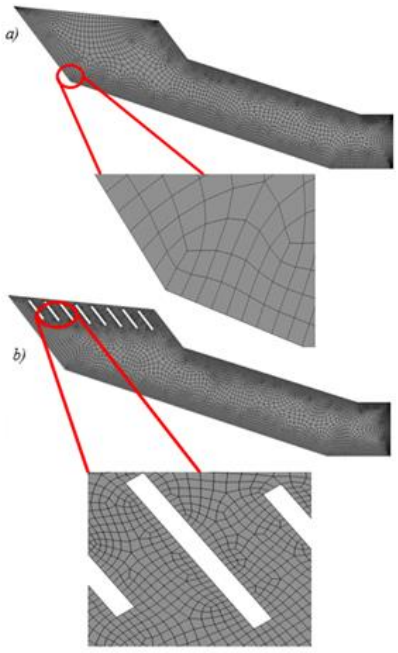

Figure 3 - Generated Mesh for the Existing Inlet System - Existing Inlet Without Inlet Screens (a) and Existing Inlet with Screens (b)

Figure 3a shows the existing inlet system without any inlet screens. The mesh has been formed using 100 elements, on both the inlet and outlet. These have been set to a bias factor of 2. This ensures that the mesh generated is refined around the wall areas. Edge sizing has also been used on each of the walls to ensure the mesh is to a high orthogonal quality. Figure 3b has been generated in an identical manner. Edge sizing has been allocated to the inlet screens with 30 divisions to ensure refinement around the area. To test the quality of these meshes the orthogonal quality was calculated. This value was calculated for the existing design with the inlet screens, and for the two design changes chosen for further analysis. The average orthogonal quality value for the three designs is 0.45754 which shows the meshes are of a suitable quality for the type of simulation.

The existing inlet screen design has been modelled successfully using SolidWorks 2016/17 from the engineering drawing provided. This was then analysed within ANSYS Fluent 15.0. The design has been simulated both with and without the inlet screens present. From this, the effect of the inlet screens upon the water flow can be analysed. Table 1 shows the maximum values obtained for the two simulations with and without the inlet screens present. From observing these results, it can clearly be seen that the inlet screens have a negative effect on several parameters. However, these inlet screens cannot be removed from the design as they are essential in preventing large debris from entering the turbine.

Table 1

Simulated Results for the Maximum Values at High Velocity for the Initial Design with and Without the Inlet Screens.

Parameters	Simulated Values	
	Without	With
Total Pressure (Pa)	439370.40	323481
Velocity Magnitude (m/s)	24.61	18.52
Turbulent Kinetic Energy (K) (m^2/s^2)	1.96	8.74
Turbulent Dissipation Rate (ε) (m^2/s^3)	4248.50	4248.50
Turbulent Intensity (%)	114.43	240.6
Turbulent Viscosity (kg/m-s)	19.30	67.31

These simulations also showed evidence that the turbulent kinetic energy is considerably large around the walls of the inlet system. The maximum value when the inlet screens are present for the turbulent kinetic energy is 8.74 [m^2/s^2]. These values were calculated using a turbulent intensity of 10 [%], as the 20 [%] intensity value only fluctuated marginally. The 10 [%] values will be used for all further analysis. The simulations in Figure 4 show where the turbulent kinetic energy is highest in the inlet system. Large amounts of turbulent kinetic energy are observed around both the inlet screens predominantly, shown as the red areas in Figure 4. However, there is also large amounts of turbulent kinetic energy which can be seen around each corner of the inlet system. This is due to the sharp corners causing vortices within the fluid which consequently is influencing the head loss. The turbulent kinetic energy here is less than around the inlet screens but still large in comparison to the amount observed in the centre of the inlet where the amount of turbulent energy is negligible. Therefore, in attempt to surpass this issue, the design modifications made focused on reducing this turbulence around the walls, to reduce the head loss from the inlet to the outlet.

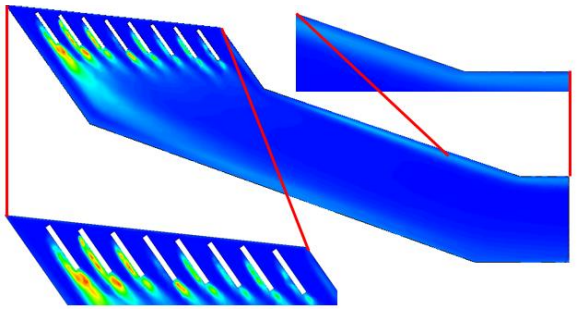

Figure 4 - Turbulent Kinetic Energy (K) Shown at Different Regions of the Existing Inlet System.

Design Modification 1

The first design modification considered is to round off the sharp corners within the existing design, creating a more curved surface. This should allow for a smooth transition of flow from the intake to the outflow towards the turbine. There were three variations of this design originally produced. Version A has rounded corners using fillets of 2 [m] for the first corners and 3 [m] in the second two corners towards the outlet. Version B incorporated fillets of 4 [m] and 5 [m] respectfully and finally Version C represents the fillets of 6m for both at the inlet and outlet sections. The maximum and minimum values were calculated for the parameters used previously at both low and high velocity water flow. Results showed that Version B improved the water flow the most, reducing vortices within the fluid. This therefore will reduce the head loss from the inlet to the outlet. This modification will therefore from this point forward be referred to as Design Change 1. A visual representation of this design change can be found in Figure 6b, with the rounded corners highlighted.

Design Modification 2

In the initial inlet system design, the mouth of the inlet is at an angle inclination of 6° from the origin, facing downstream. This has been measured using the engineering drawings. Figure 5 shows the static pressure points at the top left corner of the inlet for both the initial design and design change 2. The static pressure for the initial design is recorded as 297176 [Pa], being largely concentrated in the upper left corner. Therefore, design change 2 is to level off the inlet to an angle of 0° from the origin. From this, the static pressure is reduced to 271771.1 [Pa]. This static pressure is distributed more widely along the top edge, which will lower the total pressure loss. This would reduce the amount of head loss from the inlet to the outlet.

There have been two variations to this design produced. Version A which uses the existing design but removes the angle of inclination at the mouth. Version B incorporates the flat mouth and fillets of 2 [m] and 3 [m]. The standard parameters were calculated for each of these designs, with version B producing the most total pressure. Therefore, version B was chosen as the best design change in this modification. From this point forward when Design Change 2 is mentioned, this is referring to Version B. A visual representation of this design change can be found in Figure 6c, with the flat top highlighted.

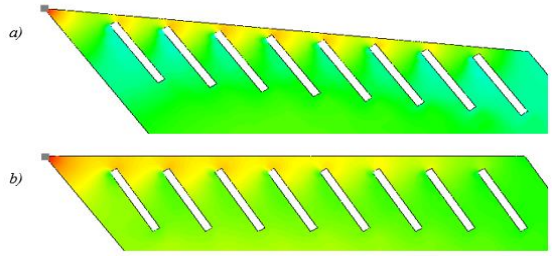

Figure 5 - Static Pressure of the Initial Design (a) and the Static Pressure of Design Change 2 (b).

Design Modification 3

The final alteration is to add a second set of inlet screens to the model. This was put into place to try and redirect the flow so that the velocity was the same throughout the entire inlet system. Two variations of this design have been modelled and tested. Version A was to add a second set of inlet screens as the flow moves around the first corner. Version B was to move the new inlet screens further down the inlet system, approximately half way. A visual representation of this design change can be found in Figure 6d.

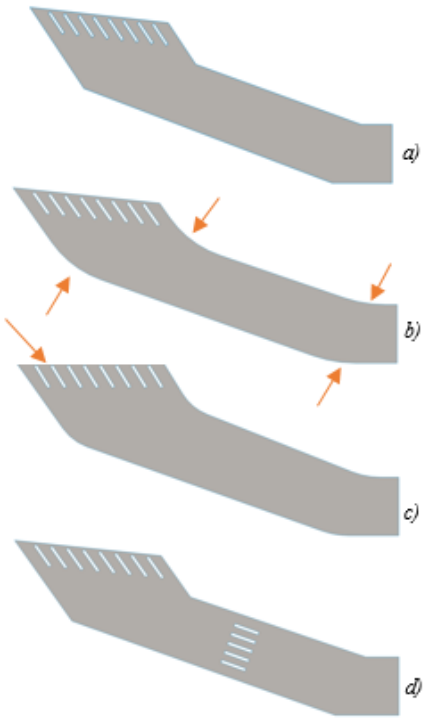

Figure 6 - A Comparison Between the Initial Design (a), Design Change 1b (b), Design Change 2b (c) and Design Change 3b (d).

Upon initial consideration of the results, design modification 3 proved to be an insufficient design change and was therefore removed from further analysis. This design change was considered

inadequate for several reasons. Firstly, because the range of total pressure values recorded was extremely large. The minimum total pressure at the higher velocity is calculated as -315894 [Pa] with a maximum total pressure of 420917.8 [Pa]. The difference between these values is too large to draw any accurate conclusions from, and therefore any results are unreliable. Secondly, this negative pressure value in reality would not be possible, because the density within the fluid would differ at different locations within the inlet system. The simulations do not allow for an accurate representation of the density fluctuations across different points. Furthermore, the velocity magnitude value was relatively high compared to the other two design changes. A velocity magnitude at the high velocity was recorded of 35.47 [m/s]. This is therefore categorised as an excessive amount to be ran through the turbine, as the speed of fluid entering the top of the turbine would be too intense for this type of technology. Additionally, the values for the area - weighted average for total pressure loss and turbulent kinetic energy were measured as drastically higher than the initial design and the two other design changes. These figures can be found in Table 3.

Design Change Review

Design changes 1 and 2 however are to be considered as possible design changes for the Ruswarp inlet system.

The maximum values for each of the measured parameters for each design change can be seen in Table 2. Looking at this table design change 1 outperforms design change 2 on several different parameters (total pressure, velocity magnitude, turbulent kinetic energy, turbulent intensity and turbulent viscosity).

Table 2

Comparison of the Maximum Values Measured at the High Velocity Flow (6.776m/s). The Different Parameters are Shown across the Initial Inlet System Design, Design Change 1 and 2.

Parameters	Inlet System Design		
	Initial	Design Change 1	Design Change 2
Total Pressure [Pa]	323481	354330.7	289891.2
Velocity Magnitude [m/s]	18.5231	20.44363	19.78837
Turbulent Kinetic Energy (K) [m^2/s^2]	8.740999	11.20539	15.60981
Turbulent Dissipation Rate (ε) [m^2/s^3]	4248.496	4248.496	4248.496
Turbulent Intensity [%]	240.6033	273.1111	319.178
Turbulent Viscosity [kg/m-s]	67.31023	72.56888	83.11087

Important values are the increase in total pressure, velocity magnitude and turbulent kinetic energy. In design change 1, the total pressure is increased compared to both the initial design and design change 2. This can be seen in Figure 7, as the total pressure in design change 1 is consistently higher across the contour intervals than the initial design. The contour intervals represent the local maximum and minimum values, with 1 being the maximum value and 41 being the minimum. Design change 2 however, does have a cross over as the lower pressures observed are higher than both the other two designs compared, but overall the average pressure value is lower.

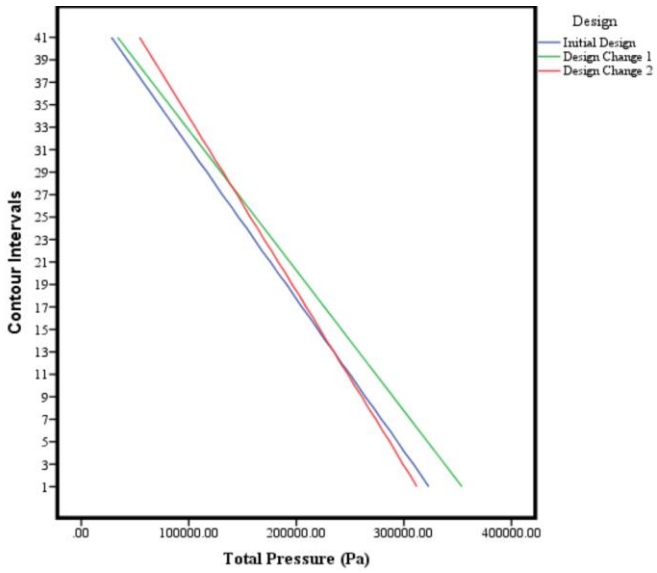

Figure 7 - Graph to show the Total Pressure Changes Across the Initial Design, Design Change 1 and Design Change 2.

This further suggests that design change 1 is favourable when looking at this specific parameter, as initially suggested by looking at Table 2. This would be an advantageous change as a higher pressure throughout the inlet system would lead to a reduction in the amount of pressure head lost at the inlet to the turbine. To further analyse this data statistical analysis was performed using the statistical analysis programme SPSS. Results were analysed using a repeated measures ANOVA to investigate the effect of design change (initial, design change 1, design change 2) on the total pressure change across the inlet system. The analysis revealed that a significant effect of design change is seen on the total pressure $F(2,38)= 39.203$, $p<0.0001$. Further analysis using LSD post hoc tests revealed this significant difference is due to a significantly higher pressure change between the design change 1 and 2 compared to the initial design ($p<0.0001$). This therefore shows that design change 1 and 2 produce a statistically higher total pressure change than the current inlet design. When comparing the results for design change 1 and 2 it is shown that design change 1 performs significantly better than design change 2 ($p=0.001$). This therefore shows that in regards to total pressure produced, that design change 1 is the better design out of the three compared.

Statistical analysis was not carried out for the inlet system design changes at the lower velocity, as the turbine is often inactive at these pressures. This is due to the river head being too low for power generation.

Therefore, the higher velocity calculations are more appropriate.

The velocity magnitude was also compared across the three designs. Design change 1 upon initial obervation for Table 2, showed the highest velocity magnitude of the three designs. This can also be seen by looking at Figure 8, where it can be seen that design change 1 has a consistently higher velocity magnitude compared to the initial design and design change 2, with the initial design being consistently lower than both modifications. This means that the flow of the water is faster through the intake system, which will in turn rotate the turbine at a higher speed, producing an increased power output.

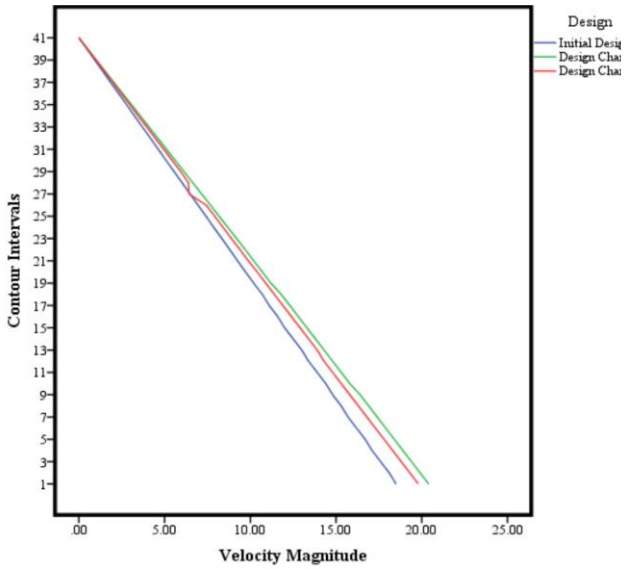

Figure 8 - Graph to show the Velocity Magnitude Changes Across the Initial Design, Design Change 1 and Design Change 2.

Further statistical analysis was carried out on this parameter. Analysis showed that there was a significant difference between velocity magnitude and design change, $F(2,38)= 110.020$, $p<0.0001$. It was then found that this significant difference was due to design change 1 producing a significantly higher velocity magnitude compared to the initial design and design change 2 ($p<0.0001$). It was also found that both design changes performed statistically better than the initial design on this specific parameter ($p<0.0001$).

The turbulent kinetic energy values were then compared. It can be seen from looking at Table 2 that both the design changes produce a higher turbulent kinetic energy than the initial design. This data can also be observed by looking at Figure 9, where the initial design is shown to have a consistently lower turbulent kinetic energy across the contour intervals, compared to the two design changes. The higher maximum turbulent kinetic energy in the design change, would result in a higher concentration of vortices around the inlet system which would possibly have a resulting effect on the turbine, as the head loss could become greater than currently observed.

These results were analysed further to see if these increases in turbulent kinetic energy were significant. If they were not significant then it could be said that the increase in turbulent kinetic energy would not have a detrimental effect on the head loss. However, statistical analysis showed that there was a significant difference in the total kinetic energy across the two designs, $F(2,38)=114.317$, $p<0.0001$. LSD post hoc analysis showed that the initial design for the inlet system had the significantly lowest total kinetic energy change, compared to design change 1. This therefore, means that the design changes would have an impact on the local maximum amount of turbulent kinetic energy produced compared to the design which is already in place.

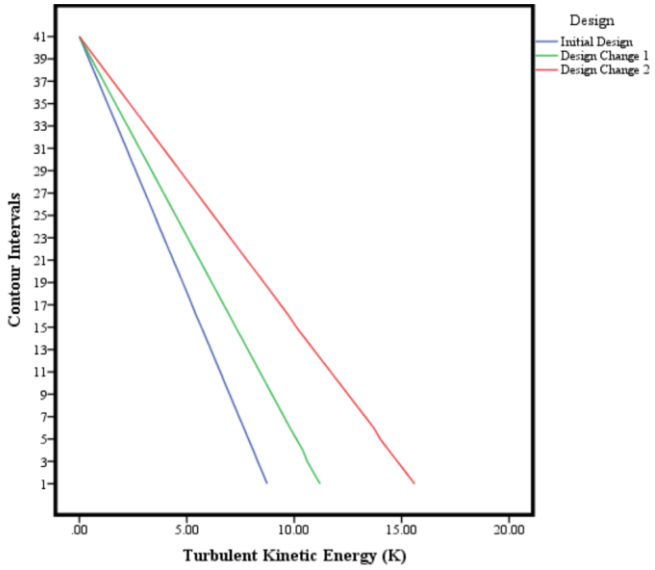

Figure 9 - Graph to show the Turbulent Kinetic Energy Changes Across the Initial Design, Design Change 1 and Design Change 2.

Table 3

Area- Weighted Average for Total Pressure Loss and Turbulent Kinetic Energy for the Initial Design, Design Change 1 and 2.

	Design			
	Initial	Design Change 1	Design Change 2	Design Change 3
	Total Pressure Loss			
Inlet	179442.11	178693.03	165336.2	220638.73
Outlet	147822.11	148103.52	147464.58	146550.64
Total	170463.59	170007.13	160261.53	199588.23
	Turbulent Kinetic Energy			
Inlet	0.6887126	0.6887126	0.6887126	0.6887126
Outlet	0.30103946	0.19083309	0.10310207	0.64935702
Total	0.57863259	0.54733938	0.52242815	0.67753059

Following on from this analysis, the area – weighted average for the design changes was calculated, which looks at the fluid flow from the inlet to the outlet.

Whereas, the previous results are the local maximum and minimum values across the designs. Table 3 shows these results, and as speculated, the turbulent kinetic energy for the design changes are lower here than in the initial design, which is not initially suggested from the local maximum and minimum values. Design change 2 shows the lowest turbulent kinetic energy value and the lowest total pressure loss throughout the intake system. The total pressure loss for design change 2 is the lowest value, due to the angle of inclination being matched with the origin at the mouth of the inlet.

V. DISCUSSION

When observing the existing intake system design, signs of turbulent flow can be seen, even without the additional assistance of computational fluid dynamics. This is the basis for the initial project hypothesis. Can the head loss entering the turbine be reduced by altering the inlet system design, and minimising the turbulent kinetic energy? Through modelling and simulating the flow of the existing design using a combination of SolidWorks 2016/17 and ANSYS Fluent 15.0 respectively, the issues with the inlet system were emphasised. The simulation showed that there were higher levels of turbulent kinetic energy around the inlet screens, and along the wall corners, influencing the pressure head loss. Therefore, the results shown in this project have outlined errors in the existing inlet system design at Ruswarp. Using the results from this project, it would be advised that a new design for the inlet system is considered. The results showed that design change 1 increased the local maximum and minimum values for each measured parameter to the greatest extent. The increase in total pressure seen will be advantageous to the fluid flow as a smaller head loss will be seen. Design change 2 also showed improvements upon the initial design, but to a lesser extent than those seen in design change 1 as only the velocity magnitude showed a positive outcome.

However, both design changes, appear to produce an increase in the maximum and minimum local turbulent kinetic energy. When looking at the results as an area - weighted average from the inlet to the outlet, a reduction in overall turbulent kinetic energy is shown in both design changes. This is because the local maximum and minimum values, are determined by the value of the contours. This means that any high or low values will have a more detrimental effect on the overall result. When considering the integral results from the inlet to the outlet, these high values have less of an impact. These results therefore indicate that the design changes do in fact reduce turbulent kinetic energy across the entire length of the system. The turbulent kinetic energy appears to be made higher at one specific contour, but overall across the inlet system the amount is reduced. Additionally, this leads to a reduction in the total pressure loss across the two design changes, ranging from the inlet to the outlet. This would indicate that the head loss would be reduced at the mouth of the turbine if the new designs were implemented.

The experimental hypothesis for the project has been met when considering the increase in total pressure. The second aspect of the experimental hypothesis has also been met as the turbulent kinetic energy is shown to be reduced when looking at the results in terms of an area – weighted average from the inlet to the outlet. However, more research may be needed to fully clarify why the local maximum points were higher than the existing design. These changes would have a significant effect on the overall head loss as opposed to the original design. Upon consideration, design change 1 has been selected as the preferred modification, as altering the inlet angle at the mouth of the intake system would be a complex and a costly modification. This may not be a financially viable option, and therefore as the two design changes appear to have similar improvements on performance, design change 1 is the favoured due to ease of implementation.

A point of consideration in the experimental design of this project, is that solely modelling the intake system, gives little information about the overall performance of the turbine. The current simulation shows the changes in various parameters within a two-dimensional schematic. This showed positive results for the changes in many parameters, and enabled observations to be made regarding improvements in the current intake system. However, this simulation does not allow for an accurate representation of how the flow will be affected through the turbine, and how the overall power output and efficiency will differentiate. The main aspect of the turbine is to generate an efficient amount of electricity; therefore, it is crucial that the intake system performs at an optimum level having a minimum amount of turbulent flow and head loss throughout. Although the current simulation does not allow for calculations showing how this fluid flow would affect power generation, it is logical to assume that an increased pressure of water through the intake system would lead to an increased power output. Additionally, from an observation of the mesh, the refinement around the inlet screens could have been improved to provide a more accurate representation of results. Due to computational time and the large amounts of simulations that had to be performed, the focus was to refine the walls to a high quality. Despite the fact that the mesh around the inlet screens was not as intended, the results still show the basis of what is occurring within the intake system, and how modifications would affect the parameters. Even though the mesh was not optimised, results still appear to validate that the modifications affect the parameters positively. The average orthogonal quality value for the three designs was calculated at 0.45754 confirming reliability.

Further research would need to be conducted which would analyse the system in its entirety. This would be achieved by modelling the intake system as well as the turbine. To accomplish this, a three-dimensional design could be created using SolidWorks 2016/17 and again, ANSYS Fluent 15.0. The main reason for not using a three-dimensional drawing of the system in

this current project is simply due to computational costs and time-scale availability. However, modelling the entire system would allow for analysis of how flow is affected across the whole intake. This will allow for calculations to determine the overall power output. A small-scale replica would also be developed and used to demonstrate the exact flow of the river entering the turbine, allowing for further analysis to the proposed design changes. CFD simulations are not 100 [%] accurate, however they do provide a visual representation of the flow movements. By creating a small replica, the flow can be visualised which will validate the CFD simulations.

To conclude, this thesis has shown that the current intake system to an Archimedes Screw Turbine in Ruswarp currently does not perform to the highest efficiency. CFD simulations of the initial design showed that this is caused due to a high total pressure loss and turbulent kinetic energy within the flow. Therefore, it is clear from the research carried out in this thesis that a modification of the design to the inlet system at Ruswarp should be considered. To resolve this issue three design changes were proposed. The changes in several various parameters were observed. Overall, this thesis has shown that by making slight adjustments to the design of the inlet system the fluid flow can be changed significantly. This shows that small modifications could be made to the design to the inlet system at Ruswarp, which would lead to a drastic change in the recorded parameters. For example, design change 1 demonstrated that by simply rounding the corners, the turbulent kinetic energy and total pressure loss can be reduced (using an area – weighted average). Therefore, if a design change was to be suggested for the inlet system for the AST at Ruswarp, design change 1 would be considered. This is due to the lower implementation cost and the improved fluid flow shown from the simulations. Overall, this thesis has shown that by modifying the original design, positive results can be demonstrated, and that if a design change was to be applied, design change 1 is suggested.

To finalise, this project has been a benchmark for what would improve the intake system of an Archimedes Screw Turbine in Ruswarp.

The author would like to thank everyone at Whitby Esk Energy for their constant support through this thesis, Dr Lian Gan for his expertise within this field of study and Miss Helen Probert for her constant support throughout.

VI. REFERENCES

[1] W. C. Turkenburg and A. Faaij, Energy and the Challenge of Sustainibility, New York: World Energy Assessment, 2000.

[2] J.-C. Sabonnadiere, Renewable Energy Technologies, New Jersey: John Wiley & Sons, 2010.

[3] D. Egre and J. C. Milewski, "The Diversity of Hydropower Projects," *Energy Policy,* vol. 30, no. 14, pp. 1225-1230, 2002.

[4] D. K. Okot, "Review of Small Hydropower Technology," *Renewable and Sustainable Energy Reviews,* vol. 26, no. 1, pp. 515-520, 2013.

[5] O. B. Haddad, M. Moradi-Jalal and M. A. Marino, "Design-operation Optimisation of Run-of-River Power Plants," *Water Management,* vol. 164, no. 9, pp. 463-475, 2011.

[6] O. Paish, "Small Hydro Power: Technology and Current Status," *Renewable & Sustainable Energy Reviews* , vol. 6, no. 6, pp. 537-556, 2002.

[7] O. Paish, "Micro-Hydropower: Status and Prospects," *Institution of Mechanical Engineers,* vol. 216, no. 1, pp. 31-40, 2002.

[8] M. Lyons and W. D. Lubitz, "Archimedes Screws for Microhydro Power Generation," in *International Conference on Energy,* Minneapolis, 2013.

[9] S. Bozhinova, V. Hecht, D. Kisliakov, G. Muller and S. Schneider, "Hydropower Converters with Head Differences Below 2.5m," *Institution of Civil Engineers,* vol. 166, no. 3, pp. 107-119, 2012.

[10] W. D. Lubitz, M. Lyons and S. Simmons, "Performance Model of Achimedes Screw Hydro Turbines with Variable Fil Level," *Journal of Hydraulic Engineering* , vol. 140, no. 10, pp. 1-11, 2014.

[11] Erinofiardi, A. Nuramal, P. Bismantolo, A. Date, A. Akbarzadeh, A. K. Mainil and A. F. Suryono, "Experimental Study of Screw Turbine Performance based on different Angle of Inclination," *Energy Procedia,* vol. 110, pp. 8-13, 2017.

[12] G. Dellinger, P. A. Garambois, M. Dufresne, A. Terfous, J. Vazquez and A. Ghenaim, "Numerical and Experimental Study of an Achimedean Screw Generator," *Earth and Environmental Science,* vol. 49, no. 10, pp. 1-10, 2016.

[13] R. Acharya, "Investigation of Differences in Ansys Solvers CFX and Fluent," Royal Institute of Technology, Stockholm, 2016.

[14] E. J. Hopfinger and G. J. F. van Heijist, "Vorticies in Rotating Fluids," *Fluid Mech,* vol. 25, pp. 241-289, 1993.

[15] P. M. Bulat and V. P. Bulat, "Comparison of Turbulence Models in the Calculation of Supersonic Separated Flows," *World Applied Sciences Journal,* vol. 27, no. 10, pp. 1263-1266, 2013.

[16] ANSYS, ANSYS Fluet Theory Guide, Canonsburg: SAS, 2013.

[17] A. Escue and J. Cui, "Comparison of Turbulence Models in Simulating Swirling Pipe Flows," *Applied Mathematical Modelling,* vol. 34, no. 10, pp. 2840-2849, 2010.

[18] T. Dutta, K. P. Sinhamahapatra and S. S. Bandyopdhyay, "Comparison of Different Turbulence Models in Predicting the Temperature Separation in a Ranque-Hilsch Vortex Tube," *International Journal of Refrigeration,* vol. 33, no. 10, pp. 789-792, 2010.

[19] E. L. Paul, V. A. Atiemo-Obeng and S. M. Kresta, Handbook of Industrial Mixing, New Jersey: John Wiley & Sons, 2004.

[20] J. E. Bardina, P. G. Huang and T. J. Coakley, Turbulence Modelling Validation, Testing and Development, California: NASA, 1997.

[21] D. C. Wilcox, "Formulation of the K-omega Turbulence Model Revisited," *AIAA Journal,* vol. 46, no. 11, pp. 2823-2838, 2008.

[22] G. C. Papageorgakis and D. N. Assanis, "Comparison of Linear and Non-linear RNG-Based K-[epsilon] Models for Incompressible Turbulent Flows," *An International Journal of Computation and Methodology,* vol. 35, no. 1, pp. 1-22, 1999.

[23] C. G. Speziale and S. Thangam, "Analysis of an RNG Based Turbulence Model for Separated Flows," NASA, Virginia, 1992.

[24] M. M. Noor, A. P. Wandal and T. Yusaf, "The Simulation of Biogas Combustion in a MILD Burner," *Journal of Mechanical Engineering and Sciences,* vol. 6, no. 1, pp. 995-1013, 2014.

VII. APPENDIX A

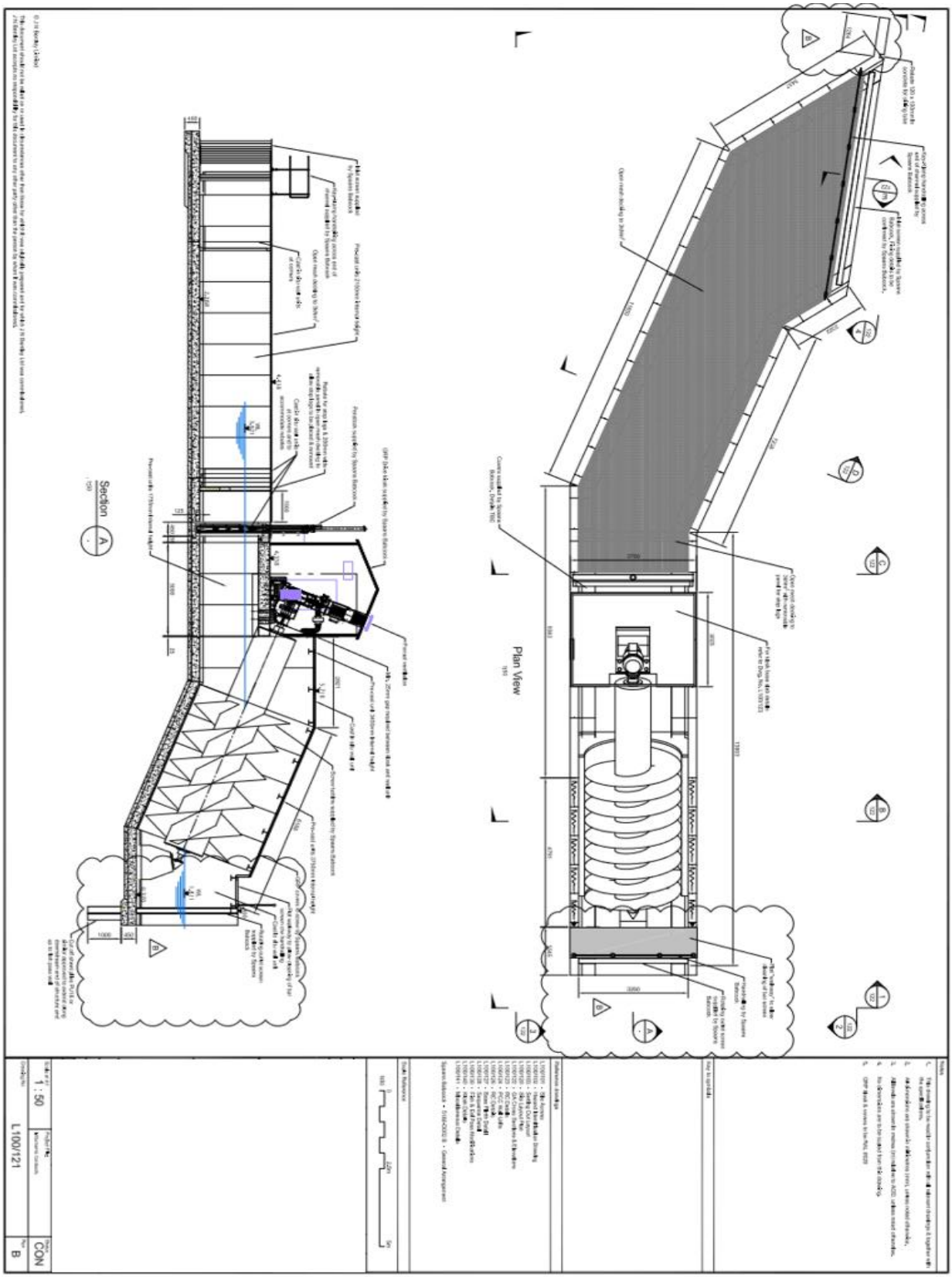

VIII. APPENDIX B